Thermal Integration of Processes With Heat Engines and Heat Pumps

An extended transportation array representation is developed for the design of process heat recovery networks incorporating heat engines and heat pumps. The formulation automatically accounts for the relocation of pinches in the integrated system. The optimal heat flow pattern is determined based on simple economic criteria. Simplified models of heat engine and heat pump systems are developed that permit integration options to be identified on the basis of heat flows without requiring specific cycle designs. The solution array identifies design alternatives and provides a decision framework to guide in selecting the final design topology.

Ross E. Swaney
Department of Chemical Engineering
University of Wisconsin
Madison, WI 53706

Introduction

The efficient utilization of thermal energy and power remains a major concern in chemical process design. The problem of process heat recovery has received considerable theoretical study, and techniques for designing optimal heat exchanger networks are comparatively well developed (Gundersen and Naess, 1988). However, the general problem is recognized to be of broader scope. Of great importance are the design options present when the thermal generation of power is permitted or required, or when refrigeration systems or other heat pumps are involved. The present paper offers a method for integrating heat engines and/or heat pumps with processes which is complementary to available techniques for heat exchanger network analysis and synthesis.

A practical assumption employed by most of the available techniques is that optimal heat recovery network designs will require the minimum utility consumption costs possible within economic minimum approach temperatures. This assumption allows the process heat flows and utility costs to be analyzed on the basis of first and second thermodynamic law requirements only, relieving the need to first postulate a specific network structure. The design task may then be approached in two stages:

1) Determining the interstream heat flow pattern(s) required to achieve minimum utility cost

2) Selecting a specific heat exchange equipment topology to accomplish the heat transfer indicated

Cerda et al. (1983) and Cerda and Westerberg (1983) showed that, for heat exchanger networks, the utility cost minimization could be formulated and solved as a "transportation problem" LP. The minimization calculation may also be performed through the familiar thermal cascade analysis and its representation as a "transshipment" LP (Papoulias and Grossmann, 1983a). However, the transportation problem representation offers several advantages to the designer during the stage of deciding network topology. The two-dimensional representation of the transportation array provides a very effective framework with which to analyze design alternatives: particular stream heat flow matches may be identified; equal-cost alternative allocations are clearly indicated; and the cost to avoid any match under consideration is displayed. This provides an organized way to arrive at a final network design while incorporating the designer's consideration of external factors impacting the design. These advantages, along with relative simplicity, carry over into the present work.

Previously, Townsend and Linnhoff (1983) discussed placement of heat engines and heat pumps relative to process heat source and sink profiles and "the process pinch." Colmenares and Seider (1987, 1989) present NLP-based procedures for integrating heat engines and heat pumps with the process thermal cascade. An important point brought forth in that work is the need to examine the economics of integrating sources and sinks with the process at all temperature levels while accounting for options to redistribute utility inputs.

With the option of adding heat engines/pumps, the concept of "the" process pinch loses its meaning: an integrated system will frequently manifest new pinches created by engine/pump placement, while the original pinch(es) may disappear. It is thus important when matching heat engine/pump sources and sinks with the process to simultaneously consider the restructuring of the heat exchange pattern among the process streams and utilities. By using heat engines/pumps, the second law consequences

of temperature are mitigated from absolute constraint to merely economic cost. Consequently, the optimal heat flow scheme is determined by economic criteria reflecting the cost of work input to the process or the value of work output.

The procedure presented here is reasonably simple, yet captures the essence of the problem: determining the economically optimal heat flows. Again it involves a decomposition involving two stages. First, the heat flow pattern between process streams, themselves, available utilities, and possible heat engine/pump sources and sinks is decided based on approximate economic cost criteria. Then, specific equipment topologies are devised to accomplish the desired heat exchange and to implement the heat engine/pump cycle(s) indicated. Justification for this decomposition is based on the premise that, for plants of reasonable scale, energy economics generally dictate cycle designs of high efficiency relative to thermodynamic limits. Consequently, it is possible to determine with reasonable accuracy work production or consumption for postulated cycles without the need to define detailed cycle structures. Costs or credits for utility and power consumption or generation thus are readily determined on the basis of given heat flows. Cycle capital costs, furthermore, tend to be dominated by turbine or compressor costs. In the absence of detailed configurational information, the cost of these machines may be estimated on the basis of work-handling capacity. It is then not unreasonable to represent cycle capital costs with a variable cost based on cycle work input or output. Heat exchange or boiler capital costs may also be assessed in a simplified manner based on heat duties.

With both utility and capital costs attributable to heat flows in the above manner, it is possible to determine the optimal heat flow pattern. The focus of this paper is on developing an extended transportation array representation with which to determine the optimal heat flows. Using that framework, the designer can identify and evaluate design alternatives and select the best structure in consideration of relevant additional factors.

In the following, simplified characterizations of real heat engine and heat pump cycles are developed to provide work coefficients relating cycle work to heat flows. The extended transportation problem formulation is presented, along with the procedure for optimizing the heat flow allocation. The approach is then illustrated with two previously studied examples.

Work Coefficients

This section develops very simple expressions for heat engine and heat pump net cycle work in terms of heat input and output flows. These expressions account for the deviation of realizable cycles from ideal Carnot efficiency, while they continue to depend predominantly on the temperatures of heat input (T^H) and rejection (T^C). The net cycle work (output) is given by

$$W = \zeta^H(T^H)Q^H - \zeta^C(T^C)Q^C \tag{1}$$

where Q^H and Q^C are the heat flows from and to the source and sink, respectively. The work coefficients $\zeta(T)$ are defined relative to a reference temperature T_0, which for convenience is usually taken as the process rejection sink temperature (e.g., cooling water temperature + approach). For ideal Carnot cycles, $\zeta^{\text{Carnot}}(T) = [1 - (T_0/T)]$. Steam turbine Rankine cycles and Rankine vapor-compression heat pump systems are treated below.

Steam Rankine cycles

Figure 1 illustrates a multilevel Rankine cycle with regenerative feed preheating. With this structure as a model, the net work output obtained from heat input at temperature level T per unit of working fluid flow may be expressed as

$$W/F = \eta_s(b^V - b^L) \cdot \frac{1}{f_{W,ph}} \tag{2}$$

$(b^V - b^L)$ is the difference at level T in the thermodynamic availability function $b = h - T_0 s$ between the steam and the returning condensate. η_s is essentially the overall isentropic efficiency of the steam turbines, η_{turbine}, modified (often insignificantly) to include the condensate pump efficiency:

$$\eta_s = \eta_{\text{turbine}} - (1 - \eta_{\text{turbine}}\eta_{\text{pump}})\left(\frac{W_{\text{pump}}/F}{b^V - b^L}\right) \tag{3}$$

The heat input at level T per unit of flow is expressed as

$$Q/F = (h^V - h^L) \cdot \frac{1}{f_{Q,ph}} \tag{4}$$

$(h^V - h^L)$ is the enthalpy difference between steam and condensate with perfect preheating. Factors $f_{Q,ph}$ and $f_{W,ph}$ adjust for the increase in Q and the slight increase in W that result because of the discrete stages and finite approach temperatures of a real preheat system. The net effect on the work coefficient is given by their ratio $\eta_{ph} = (f_{Q,ph}/f_{W,ph})$. Net preheat losses in the range of 2–4% appear typical.

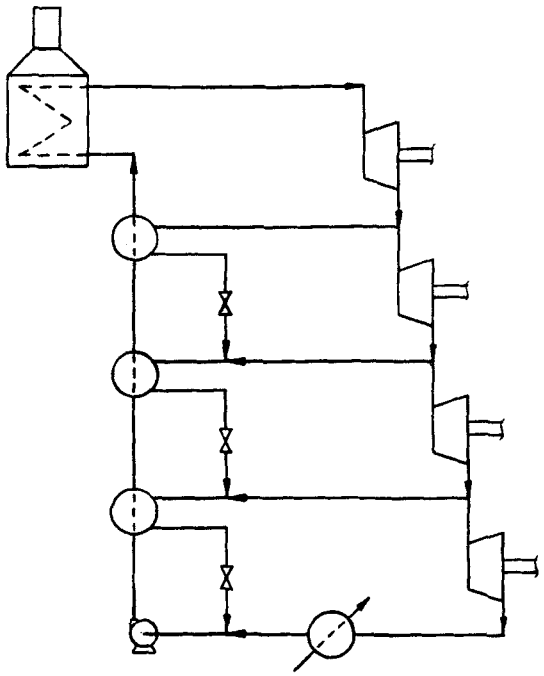

Figure 1. Multilevel Rankine cycle with regenerative feed preheating.

Combining Eqs. 2 and 4 produces the desired work coefficient

$$\zeta(T) = \eta_s \eta_{ph}\left[1 - \frac{T_0}{\hat{T}}\right] \tag{5}$$

where

$$\hat{T}(T, P) = \frac{h^V - h^L}{s^V - s^L} \tag{6}$$

Thermodynamic functions for the steam $(\cdot^V)$ are evaluated at temperature T and the stipulated pressure P (saturated or superheated). The condensate $(\cdot^L)$ is evaluated as saturated liquid at the same pressure P.

The function $\hat{T}(T, P)$, the Carnot equivalent temperature, is displayed in Figure 2 for steam. Note that for saturated steam $\hat{T} = T$, whereas superheated conditions entail a thermodynamic efficiency loss evidenced by $\hat{T} < T$. Limitations on the permissible moisture content at turbine exhaust conditions generally impose superheat requirements. (Maximum limits of 10–15% moisture are typical for conventional machines.) For a chosen exhaust temperature and moisture content, the trajectory of steam superheat conditions vs. temperature is fixed for a given turbine efficiency (see Appendix A.) Figure 3 displays the family of such trajectories. If no liquid separation between stages is employed, the final exhaust temperature T_0 will define the trajectory; otherwise, the exhaust temperature of the first wet stage governs. Once the trajectory position is established, the dependence of $\hat{T}$ on T is readily obtained from Figure 3 or analogous calculation. It should be noted that turbine materials considerations conventionally limit steam temperatures to a maximum of $\approx$1,000°F = 811 K.

Work coefficients $\zeta^H(T^H)$ for heat input at temperature T^H are evaluated as above with the steam temperature T equal to T^H. Work coefficients $\zeta^C(T^C)$ for heat rejection at temperature T^C are evaluated in the same manner, except that T^C corresponds to saturation conditions, and $\hat{T}$ is computed for steam conditions along the trajectory at the pressure required for saturation at T^C. Figure 4 displays $\hat{T}$ directly in terms of $T^C = T^L$ given the temperature T_{sat} at which the steam trajectory reaches

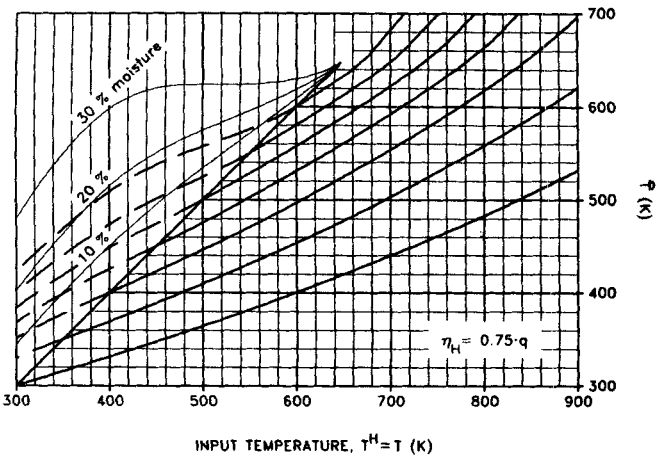

Figure 3. Expansion trajectories based on input temperature.

saturation. Both procedures assume that no advantage can be taken of the nonconstant source and sink temperature profiles for superheated steam. A set of approximate equations for estimation of $\hat{T}$ from T^C and T^H is presented in Appendix B.

Rankine cycle heat pumps

The following estimation procedure for refrigeration or heat pump systems assumes that an appropriate multilevel compound or cascade system will be employed with suitably chosen refrigerant(s). We make two assumptions:

1) The actual work required for each component cycle is related to the reversible work by

$$\frac{W_i}{Q_i^C} = \frac{1}{\eta_c}\left[1 - \frac{T_{i-1}}{T_i}\right] \tag{7}$$

where the cycle efficiency η_c is taken to be the same for each level.

2) The temperature levels are spaced at the constant ratio

$$\frac{T_{i-1}}{T_i} = \rho > 1 \tag{8}$$

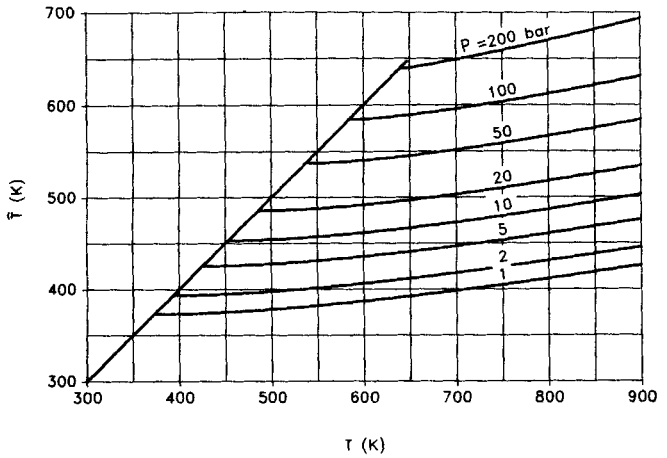

Figure 2. Rankine cycle Carnot equivalent temperature for steam.

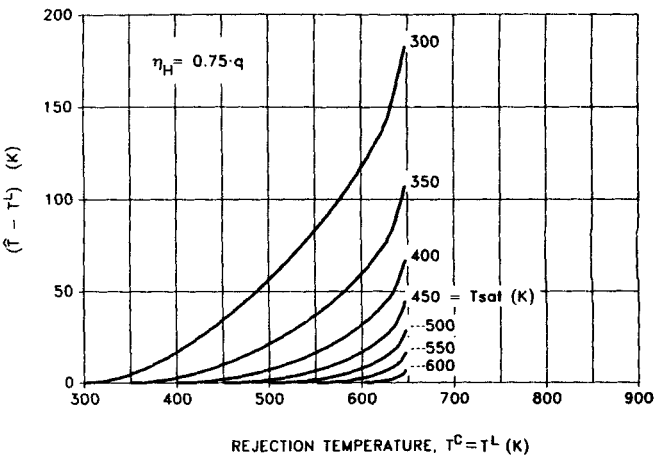

Figure 4. Expansion trajectories based on rejection temperature.

Equations 7 and 8 lead to a simple difference equation whose solution yields the following expression for the work coefficient for the coupled cycles:

$$\zeta(T) = 1 - \left(\frac{T_0}{T}\right)^m \tag{9}$$

where

$$m = \frac{\ln\left[1 + \dfrac{\rho - 1}{\eta_c}\right]}{\ln \rho} \tag{10}$$

The parameter ρ has only very minor influence in Eq. 10 for the range of typical values (say 1.05–1.2) and a rough estimate will suffice. The cycle efficiency $\eta_c = \eta_R \cdot \eta_I$ reflects irreversibilities in both compression and expansion. Its value will depend on compressor type, working fluid, and other cycle details, though for well-designed systems the range of variation is not great. η_R reflects irreversibilities imposed by the Rankine cycle topology itself. Estimates may be inferred easily from previous designs, with typical values lying in the range of 0.80 to 0.95. η_I denotes the isentropic efficiency of the compressor and will typically lie in the range 0.75 to 0.85 for larger units.

A completely analogous result may be developed for coupled Rankine cycle heat engines of most applicability to systems operating well below the critical region, with no superheating or regenerative preheating:

$$\zeta(T) = 1 - \left(\frac{T_0}{T}\right)^{m'} \tag{11}$$

$$m' = \frac{\ln\left[1 - \eta_c' \dfrac{(\rho - 1)}{\rho}\right]}{\ln \rho} \tag{12}$$

η_c' is again a per-cycle efficiency, with temperature level spacing given by $\rho = (T_j/T_{j-1}) > 1$.

Equations 5, 9 and 11 provide a simple means of estimating heat engine/pump net work as a function of heat input and rejection flows. These work coefficients will allow the consequences of process-engine or process-pump heat allocation decisions to be examined while keeping the design of cycle details an implicit task.

Extended Transportation Array

Here the transportation array representation for heat matches among process streams and utilities presented by Cerda et al. (1983) is extended to include matches between process streams, utilities, heat engine/pump input sinks and rejection sources, and power utility input or output. Note that the terms "cold stream" and "hot stream" include both the process streams and the cooling or heating utilities unless further qualified.

We begin by dividing the process streams into temperature intervals in the conventional manner: minimum approach temperature contributions $\Delta T_{\min,k}$ and $\Delta T_{\min,l}$ are assigned to each cold stream k and hot stream l, respectively, to insure that in a heat exchange between k and l the minimum approach temperature will not be less than $(\Delta T_{\min})_{k,l} = (\Delta T_{\min,k} + \Delta T_{\min,l})$. Then, the set of candidate pinch points is formed by including the inlet and outlet temperatures of each cold stream k, increased by $\Delta T_{\min,k}$, and the inlet and outlet temperatures of each hot stream l, decreased by $\Delta T_{\min,l}$. This set of temperatures specifies the dividing points defining the n temperature intervals. The outlet temperatures are included also as candidate pinch points, because heat engine/pump sources and sinks will be postulated at these temperatures. (In special cases having large unbroken temperature spans, it sometimes will be desirable to introduce extra interval divisions to provide for more integration possibilities.) The heat duties ΔH_{ki} for each cold stream k in each interval i are computed by subdividing the stream enthalpy at the interval dividing temperatures, decreased by $\Delta T_{\min,k}$. The heat duties ΔH_{lj} for each hot stream l in each interval j are likewise computed by subdividing at the interval temperatures, increased by $\Delta T_{\min,l}$.

The composite process heat duties for each interval may then be computed:

$$a_i = \sum_{k \in \left\{\begin{smallmatrix}\text{cold}\\ \text{process}\\ \text{streams}\end{smallmatrix}\right\}} \Delta H_{ki} \quad i = 1, \ldots, n \tag{13}$$

$$b_j = \sum_{l \in \left\{\begin{smallmatrix}\text{hot}\\ \text{process}\\ \text{streams}\end{smallmatrix}\right\}} \Delta H_{lj} \quad j = 1, \ldots, n \tag{14}$$

The lumping of all cold process streams and hot process streams into single cold and hot composites produces a problem formulation of the smallest size. Options exist to maintain the interval heat duties for each stream as segregated quantities as in the original formulation of Cerda et al. (1983) or to use any intermediate degree of selective segregation. Appropriate segregation will be required either when particular stream matches are to be prohibited or when different stream matches within an interval are to be assigned different costs. The development to follow may be used with any desired aggregation scheme by including distinct interval heat duties a_i or b_j for each distinct stream composite.

The heating and cooling utilities are not aggregated with the process streams, since matches with them are assessed as particular unit costs. Instead, for each cooling utility there is associated a supply capacity $a_i, i = n + 1, \ldots, N$, and for each heating utility a supply capacity $b_j, j = n + 1, \ldots, M$. The values a_i and b_j specify consumption limits for those utilities with constrained supplies.

With the interval heating and cooling duties for all cold and hot streams defined by $\{a_i, i = 1, \ldots, N\}$ and $\{b_j, j = 1, \ldots, M\}$, the transportation array may be assembled as depicted in Figure 5. Each cell in the array corresponds to a possible heat flow from a heat source to a heat sink. The quantity of heat flow from hot stream source b_j to cold stream sink a_i will be denoted by q_{ij}. The cells corresponding to these flows form the part of the array originally presented by Cerda et al. (1983). Though not strictly necessary, it is advantageous to order the rows and columns heuristically as related by Cerda et al.: with those heat flows that are infeasible due to either thermodynamics or match prohibition "crossed out," order the process streams first by row and then by column to get the most number of infeasible cells near the top and right. Columns for heating utilities are included at the right with cooling utilities at the bottom. (The utility row for

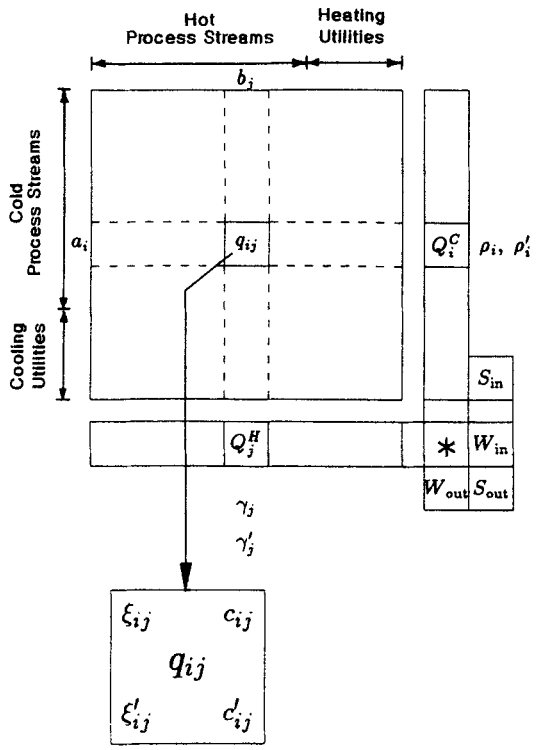

Figure 5. Cell arrangement in transportation array.

the process rejection sink i_0 also contains the S_{in} cell, as explained below.) Within this structuring, rows and columns are arranged in the order of increasing cost.

The original array is extended by appending a row of cells for flows Q_j^H into the heat engine/pump system from each hot stream source j. Likewise, a column is added for heat flows Q_i^C rejected to each cold stream sink i. There are also several special cells appearing in the bottom right corner of Figure 5. W_{in} and W_{out} correspond to net work into or out of the heat engine/pump system. S_{in} and S_{out} represent nonphysical "slack" flows whose values denote unused work import and export capacities. When total work import is not constraining, S_{in} may be replaced with an asterisk; and when neither work import nor work export is constraining, both S_{in} and S_{out} may be replaced with asterisks. Asterisks denote "tie" cells that do not represent physical flows, but do function as "active" cells in the procedures below. When a heating and cooling utility pair both have unconstrained supplies, their intersection flow q_{ij} may likewise be replaced with an asterisk.

The appended cells may each be assigned row and column indices i and j, though the special symbols for their flows given above will be retained for clarity. All cells in the array contain the same elements: q_{ij} (or Q_i^C, Q_j^H, W_{in}, W_{out}, S_{in}, S_{out}) denotes the energy flow allocation from column j to row i, and is placed in the center of the cell. The cell corners hold up to four entries: c_{ij}, ξ_{ij}, c_{ij}', ξ_{ij}' positioned as in Figure 5. (Zero-valued entries may be left blank.) The entry c_{ij} for the cell specifies the cost per unit flow for the cell and is determined from

$$c_{ij} = c_{ij}^0 + c_{ij}'w \tag{15}$$

The multiplier w (determined below) provides the cost per unit of incremental work used or produced by the process. Constant c_{ij}' specifies the net work input required per unit of heat flow, while c_{ij}^0 specifies all other costs to be assessed per unit of flow.

Cost coefficients for the different types of cells are determined as indicated in Table 1. The work coefficients ζ_i^C and ζ_j^H are evaluated at temperatures T_i^C and T_j^H obtained by increasing or decreasing each corresponding interval temperature by an appropriate ΔT_{min} contribution. In addition to the heating and cooling utility consumption costs c^{Util}, work import cost c_{in}^W, and work export value c_{out}^W, cost factors c_i^C and c_j^H may be specified for the heat engine/pump heat flows in order to include incremental capital costs for the heat engine/pump system. Using a simple fixed-plus-variable capital cost model,

$$\text{(capital cost)} = k_0 + k_W \cdot \text{(work output or input)} + k_Q \cdot \left(\sum_j Q_j^H + \sum_i Q_i^C\right) \tag{16}$$

appropriate cost coefficients are given by

$$\left.\begin{aligned} c_i^C &= -\zeta_i^C k_W + k_Q \\ c_j^H &= \zeta_j^H k_W + k_Q \end{aligned}\right\} \text{heat engines} \tag{17a, b}$$

$$\left.\begin{aligned} c_i^C &= \zeta_i^C k_W + k_Q \\ c_j^H &= -\zeta_j^H k_W + k_Q \end{aligned}\right\} \text{heat pumps} \tag{18a, b}$$

These approximations are serviceable, because the dominant capital cost will generally lie in the turbines or compressors, whose costs correlate with power capacity. It also is possible to employ a schedule of cost coefficients that vary according to temperature level. This would be appropriate, for instance, to account for the higher costs of low-pressure operation when specific volumes become large.

From Table 1, it is clear that when determining c_{ij}^0 and c_{ij}' for the Q_i^C and Q_j^H cells, the work coefficients $\zeta(T)$ and the cost factors k_W and k_Q require an *a priori* decision that each cell belongs either to a heat engine or a heat pump system. Ordinarily this is not a problem, since a heat engine and heat pump both operating together with overlapping temperature ranges should normally not be economically favorable. If both heat engines and pumps are to be considered and it is not clear *a priori* which temperature intervals are appropriate for each, a viable procedure is to include a separate Q_i^C column and Q_j^H row for each system. Each system will have its own W_{in}, W_{out}, and tie cell, but will not share

Table 1. Cell Cost Coefficients

	Cell Type	c_{ij}^0	c_{ij}'
q_{ij}	process → process	—	—
q_{ij}	process ↔ utility	c^{Util}	—
q_{ij}	utility → utility	—	—
Q_i^C	heat engine/pump rejection → process	c_i^C	ζ_i^C
Q_i^C	heat engine/pump rejection → utility	$c_i^C + c^{Util,i}$	ζ_i^C
Q_j^H	process → heat engine/pump input	c_j^H	$-\zeta_j^H$
Q_j^H	utility → heat engine/pump input	$c_j^H + c^{Util,j}$	$-\zeta_j^H$
W_{in}	import work → heat engine/pump input	c_{in}^W	-1
W_{out}	heat engine/pump output → work export	c_{out}^W	$+1$
S_{in}	work import slack	—	—
S_{out}	work export slack	—	—

cells with the other. The heat flow optimization will then consider both systems at each temperature without prejudice.

Cell entries ξ_{ij} and ξ'_{ij} are determined during the course of the optimization procedure.

Optimizing Heat Flows

With the array constructed, the economically optimal heat flow allocation is determined in three stages:

I. Initial allocation

II. Primal phase

III. Dual phase

The initial allocation provides a feasible heat balance to use as a starting point. The heat flows are then optimized through a series of steps in which heat duties are shifted around loops in a manner which preserves heat balance. In the primal phase, the heat flows are optimized under an initial estimate of the work cost multiplier w. The dual phase completes the optimization by revising w to its correct value as needed. The corresponding procedures are outlined below. The mathematical basis for them will be described in the section to follow.

Initial allocation

Here we employ the "northwest corner" algorithm. Allocations are entered into cells starting in the upper left corner and proceeding from left to right, down the array. When completed, the sum of the allocations in each row and column will equal a_i and b_j. A column sum U_{in} or row sum U_{out} may be specified for the work import column and work export row, if limits are imposed on these quantities. Rows or columns containing an asterisk have no required sum. The Q_i^C column sum, however, must be made equal to the Q_j^H row sum to set an initial energy balance on the heat engine/pump system.

The allocation obtained must satisfy the following property: Each nonzero cell must complete the total sum for either its row or its column. The procedure is thus to enter into each cell that amount required to complete its row sum or column sum, whichever requires the smaller amount. Infeasible cells receive no entries, but asterisks are treated as nonzero entries.

Primal phase

The heat flow pattern is optimized by shifting duty into an "inactive" cell and out of one that is currently "active." Active cells consist of those currently having nonzero flows, as well as the asterisk cells, which are permanently active. The inactive cell to become "entering" is selected on the basis of cell entries ξ_{ij} and c_{ij}. The value ξ_{ij} computed below is the cost advantage to the rest of the network of supplying heat to shift into the cell, while c_{ij} is the cell's cost of taking the heat load on. Since total cost is to be minimized, cells having $c_{ij} < \xi_{ij}$ indicate an advantageous redistribution and are appropriate entering cells.

The shifting takes place via the unique "loop" that may be formed with the entering cell. The loop follows a path of horizontal and vertical steps preceeding from the entering cell, through the array, and back to the entering cell using only active cells as turning points. These active cells are "signed" alternately ⊖ and ⊕, with the entering cell signed ⊕. To shift the heat duty, the flows in the signed cells are each either increased (if ⊕) or decreased (if ⊖) by the same amount. Since every row and column involved will have exactly one ⊕ and one ⊖ cell, row and column heat balances are maintained during the shift.

Heat loads are shifted around the loop until one of the flows signed ⊖ is reduced to zero. This "leaving" cell is identified as that ⊖ cell having the smallest previous flow, q_{min}. The shift moves q_{min} units of heat around the loop, and the cell becomes inactive.

A series of heat redistribution shifts are performed until no advantageous ($c_{ij} < \xi_{ij}$) shifts remain. Note that all cells take part in the procedure identically, including the work and slack flows. The procedure (the "stepping stone" algorithm) is summarized:

Step 0. Estimate w. Compute c_{ij} for each cell from Eq. 15.

Step 1.

a) Compute row multipliers ρ_i and column multipliers γ_j such that

$$\rho_i + \gamma_j = c_{ij} \tag{19}$$

for every *active* cell in the array:

0) Assign $\rho_{i_0} = 0$ for the process heat rejection utility (at T_0).

1) For each row with an assigned ρ_i, for each active cell in the row assign the column multiplier γ_j computed from Eq. 19.

2) For each column with an assigned γ_j, for each active cell in the column assign the row multiplier ρ_i computed from Eq. 19.

3) Continue 1) and 2) until all ρ_i, γ_j are computed.

b) For every *inactive* cell, compute $\xi_{ij} = \rho_i + \gamma_j$.

Step 2. Identify active cells having $c_{ij} < \xi_{ij}$.

a) If no $c_{ij} < \xi_{ij}$, stop. (Primal phase is complete.)

b) Otherwise, select an entering cell. Select largest $(\xi_{ij} - c_{ij})$ or choose arbitrarily.

Step 3. Identify loop for entering cell.

Step 4. Shift q_{min} around loop.

Step 5. Repeat from step 1.

Dual phase

This procedure adjusts the value of w based on the quantity

$$S = -\sum_j \zeta_j^H Q_j^H + \sum_i \zeta_i^C Q_i^C - W_{in} + W_{out} \tag{20}$$

and the cell parameters c_{ij}, ξ_{ij}, c'_{ij} $(=dc_{ij}/dw)$, and ξ'_{ij} $(=d\xi_{ij}/dw)$. Heat loads are shifted around loops until $S = 0$, at which point the heat flow allocation is then optimal.

A final test is then performed to verify that no portion of a heat engine (pump) system is operating in reverse as a heat pump (engine). At each temperature level T_k, the net heat flow R_k down (heat engines) or up (heat pumps) must be nonnegative:

$$R_k = \sum_{T_j^H \geq T_k} (1 - \zeta_j^H) Q_j^H - \sum_{T_i^C \geq T_k} (1 - \zeta_i^C) Q_i^C \geq 0 \quad \text{(heat engines)} \tag{21}$$

$$R_k = \sum_{T_j^H \leq T_k} (1 - \zeta_j^H) Q_j^H - \sum_{T_i^C \leq T_k} (1 - \zeta_i^C) Q_i^C \geq 0 \quad \text{(heat pumps)} \tag{22}$$

If a flow reversal is detected, the engine/pump system is par-

titioned into two separate systems, with one operating only over temperatures above the interval of greatest violation in Eq. 21 or 22, and the other operating only over temperatures below. The two systems are given a single feasible cell in common to allow heat to cascade from one to the other in the permissible direction only. Feasible allocations are made into the revised array structure and the Primal Phase is resumed.

Step 0. Use a primal phase solution as starting point.

Step 1. Compute S from Eq. 20.

Step 2. Compute quantities ρ_i, γ_j, and ξ_{ij} based on c_{ij} using the step 1 procedure of "primal phase."

Step 3. Compute quantities ρ'_i, γ'_j, and ξ'_{ij} based on c'_{ij} using a procedure completely analogous to step 1 of "primal phase" i.e., for *active* cells obtain

$$\rho'_i + \gamma'_j = c'_{ij} \tag{23}$$

while for *inactive* cells compute $\xi'_{ij} = \rho'_{ij} + \gamma'_{ij}$, with $\rho'_{i_0} = 0$ for the process heat rejection utility.

Step 4. Identify those inactive cells having

$$\begin{cases} \xi'_{ij} > c'_{ij} & (\text{if } S > 0) \\ \quad \text{or} & \\ \xi'_{ij} < c'_{ij} & (\text{if } S < 0) \end{cases}$$

a) Among these determine the cell $(\hat{\imath}, \hat{\jmath})$ having the minimum absolute value for the ratio

$$(\Delta w)_{ij} = \frac{c_{ij} - \xi_{ij}}{\xi'_{ij} - c'_{ij}} \tag{24}$$

b) Adjust w by the amount $(\Delta w)_{\hat{\imath}\hat{\jmath}}$ and recompute c_{ij} from Eq. 15. Cell $(\hat{\imath}, \hat{\jmath})$ becomes the entering cell.

Step 5. Identify loop for entering cell.

Step 6.

a) Determine $q_{\min}$ for the loop.

b) Compute $q_S = S/(\xi'_{ij} - c'_{ij})$.

c) if $q_S < q_{\min}$, shift q_S around the loop. Allocation is then optimal. Perform flow reversal check using Eq. 21 or 22. Stop.

d) Otherwise, shift $q_{\min}$ around loop.

Step 7. Repeat from step 1.

Comments

In practice, w seldom requires extensive adjustment, and the "dual phase" is quite short. In many cases the value of w will be close to either $(c^W_{\text{in}} + c^{\text{Util},i_0})$ or $(-c^W_{\text{out}} + c^{\text{Util},i_0})$, so one of these values provides an excellent starting estimate.

It may be advantageous to apply the above procedure in the following sequence:

1. Perform the "initial allocation" to the entire array.

2. Perform the "primal phase" first on the original part of the array only, ignoring the heat engine/pump system cells. This preliminary result gives a reference cost without heat engine/pump integration.

3. Perform the "primal and dual phases" on the entire array. Alternatively, the three stages may be applied directly to the entire array.

After solution, a heat flow allocation minimizing the cost function is given by the heat duties in the active cells. The final array, however, contains much additional information. After computing updated values for ξ_{ij}, for each inactive cell the quantity $p_{ij} = (c_{ij} - \xi_{ij})$ gives the incremental cost of shifting heat load into that cell. Four uses are apparent:

1. Cells having $c_{ij} = \xi_{ij}$ indicate equal cost alternative solutions.

2. The incremental cost per unit to force a particular flow match is given by p_{ij}, i.e., the cost penalty p_{ij} must be subtracted from coefficient c_{ij} in order to make the cell become an entering cell.

3. The incremental cost per unit to avoid (force flow out of) a current match is given by the smallest penalty p_{ij} among those inactive cells with loops containing the current match as a $\ominus$ cell. (These may be located by working backwards from the active cell.)

4. The incremental cost per unit to increase the flow in a current match is given by the smallest penalty p_{ij} among those inactive cells with loops containing the current match as a $\oplus$ cell.

The correspondingly modified allocations may be obtained by altering the selected cost coefficient by the required penalty and resuming the primal and dual phases to shift the heat loads and reoptimize the rest of the array as needed. It may be necessary to repeat the process until the entire quantity of heat flow is shifted as desired. Usually, however, the additional effort needed to examine such alternatives is small, and often questions may be answered by inspection.

Sensitivity of the optimum allocation to uncertainties and variations in the cost coefficient components c^0_{ij} and ζ^C_i, ζ^H_j is also easily examined. To be significant, coefficient variations must be large enough to cause an inactive cell to become "entering"; for smaller variations the optimal allocation pattern will not change.

A useful application of these procedures is the following method of dealing with nonlinear cost-capacity relationships: Assuming a cost relationship is concave, the fixed-plus-variable cost model may be fitted at a given capacity with a tangent line. The variable cost (e.g., k_W) is taken as the marginal cost (slope) at the assumed capacity, and the fixed charge (k_0) is the resulting intercept.

1) Optimize flows using the marginal cost at the largest anticipated capacity (cost will be optimistic).

2) Increase the marginal cost to that for the actual capacity at the solution. Reoptimize flows and iterate on this step if necessary.

3) Verify that the remaining fixed charge is less than the cost to eliminate the item entirely. If not, then eliminate. This method will also allow the proper consideration of costs for combined turbine designs employing multiple stages within the same casing or on a common shaft.

Table 2. Annualized Capital Cost Contributions

Equipment	Annualized Capital Cost \$/kW
Steam turbines (k_W)	18
Refrigeration/heat pump (k_W)	150
Boiler (absorption duty)	22
Heat exchangers	6
Condenser (water cooled)	15

Table 3. Annualized Utility Costs

Utility	Conditions	Annual Cost $/kW
Boiler (absorption duty)		109
HP Steam	672 K, 69 bar	104
MP Steam	605 K, 17.2 bar	73
LP Steam	411 K, 3.5 bar	56
Electrical power (purchase)		440
Electrical power (sale)		−320
Cooling water		6

Table 4. Heating and Cooling Requirements for Example 1

Stream	Initial Temp. K	Final Temp. K	Duty MW
H1	600	310	261
H2	440	320	5.9
H3	387	310	2.8
H4	325	325	65
H5	353	353	171
H6	600	600	18
C1	440	600	142
C2	315	440	105
C3	371	371	119
C4	387	387	91

Basis of Procedure

The optimization procedure solves the following linear program in the variables q_{ij}, Q_i^C, Q_j^H, W_{in}, W_{out}, S_{in}, S_{out}:

$$\min \sum_{i=1}^{N}\sum_{j=1}^{M} c_{ij}^0 q_{ij} + \sum_{i=1}^{N} c_i^C Q_i^C + \sum_{j=1}^{M} c_j^H Q_j^H + c_{in}^W W_{in} + c_{out}^W W_{out} \quad (25)$$

$$\text{s.t.} \quad \sum_{j=1}^{M} q_{ij} + Q_i^C = a_i \quad (i = 1, \ldots, N, i \neq i_0) \quad (26)$$

$$\sum_{j=1}^{M} q_{i_0 j} + Q_{i_0}^C + S_{in} = a_{i_0} \quad (i_0 = \text{process rejection sink}) \quad (27)$$

$$\sum_{i=1}^{N} q_{ij} + Q_j^H = b_j \quad (j = 1, \ldots, M) \quad (28)$$

$$S_{in} + W_{in} + S_{out} = U_{in} \quad (29)$$

$$W_{out} + S_{out} = U_{out} \quad (30)$$

$$\sum_{j=1}^{M} Q_j^H + W_{in} + t = 0 \quad (31)$$

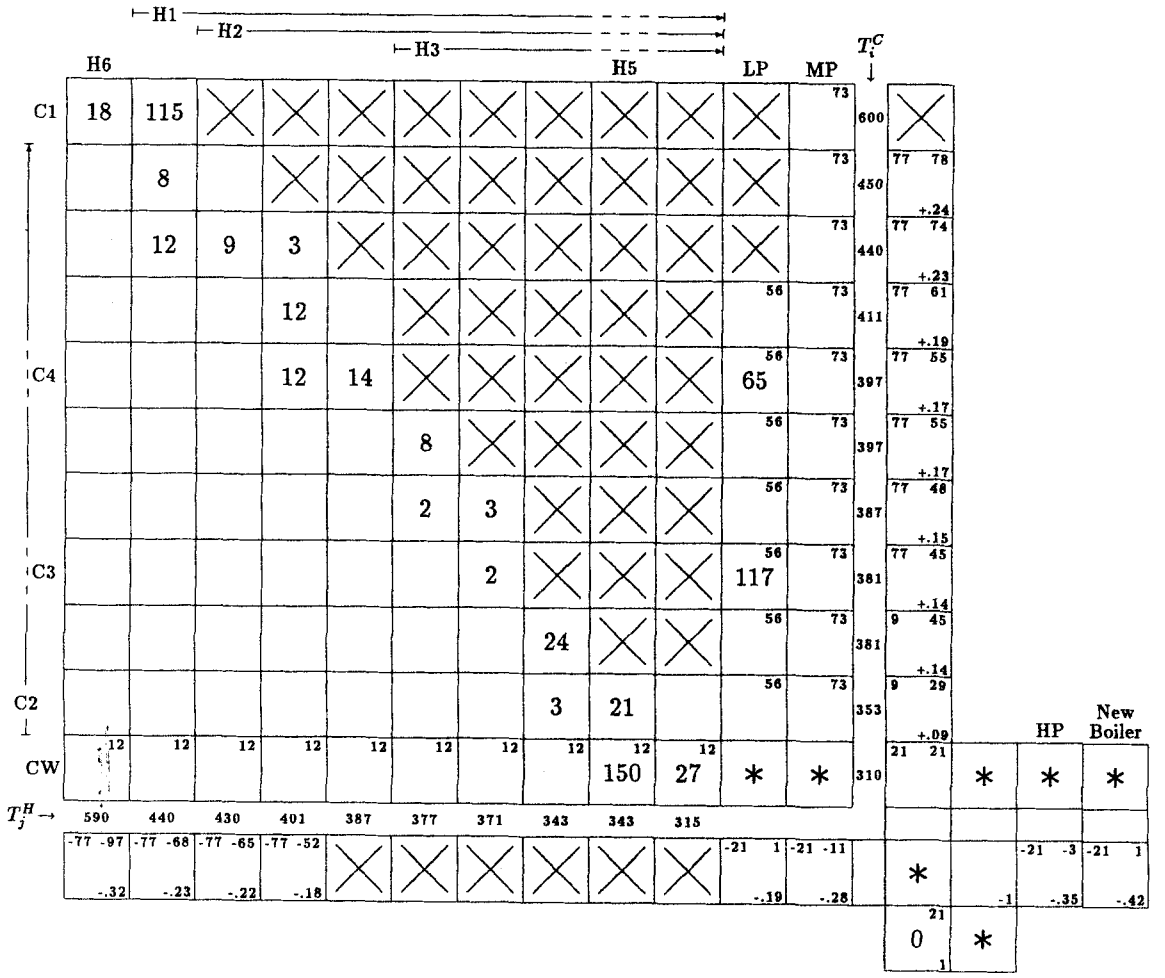

Figure 6. Example 1 initial allocation.

$$\sum_{i=1}^{N} Q_i^C + W_{out} + t = 0 \tag{32}$$

$$\sum_{j=1}^{M} \zeta_j^H Q_j^H - \sum_{i=1}^{N} \zeta_i^C Q_i^C + W_{in} - W_{out} = 0 \tag{33}$$

$$q_{ij}, Q_i^C, Q_j^H, W_{in}, W_{out}, S_{in}, S_{out} \geq 0$$
$$(i = 1, \ldots, N; j = 1, \ldots, M) \tag{34}$$

This program is not in the form of a "transportation problem," but could easily be dispatched in black-box fashion with standard simplex method software. However, the representational advantages of the transportation array may be retained as follows.

With the exception of constraint 33, the rest of Eqs. 25–34 constitutes a transportation problem. We therefore employ a Lagrangian relaxation of Eqs. 25–34, omitting constraint 33, where the objective function becomes

$$\min \sum_{i=1}^{N} \sum_{j=1}^{M} c_{ij}^0 q_{ij} + \sum_{i=1}^{N} (c_i^C + w\zeta_i^C) Q_i^C + \sum_{j=1}^{M} (c_j^H - w\zeta_j^H) Q_j^H + (c_{in}^W - w) W_{in} + (c_{out}^W + w) W_{out} \tag{35}$$

The resulting transportation problem given by Eqs. 35, 26–32, 34 is solved during the Primal Phase. With minor variations, the solution procedure employed is conventional and is explained in standard refernces on linear programming (e.g., Murty, 1983).

The quantity S given by Eq. 20 measures the violation of the relaxed constraint. The dual phase adjusts w until Eq. 33 is satisfied while maintaining primal optimality. LP duality theory provides that the original LP will be solved when the restricted dual function is maximized over w, and that S is the corresponding reduced gradient of the dual function with respect to w. The Dual Phase presented moves w in the reduced gradient direction, stepping through a series of adjacent vertex points. Since the dual function is concave in a single variable, the solution is attained monotonically in a finite number of steps. Each adjacent vertex presents a degenerate relaxed primal solution, at which heat loads are shifted to maintain optimality of the relaxed primal. On termination, the shift of q_S provides feasibility for the unrelaxed problem.

Examples

The following two examples illustrate how the procedure is applied to integrated power recovery and refrigeration/heat

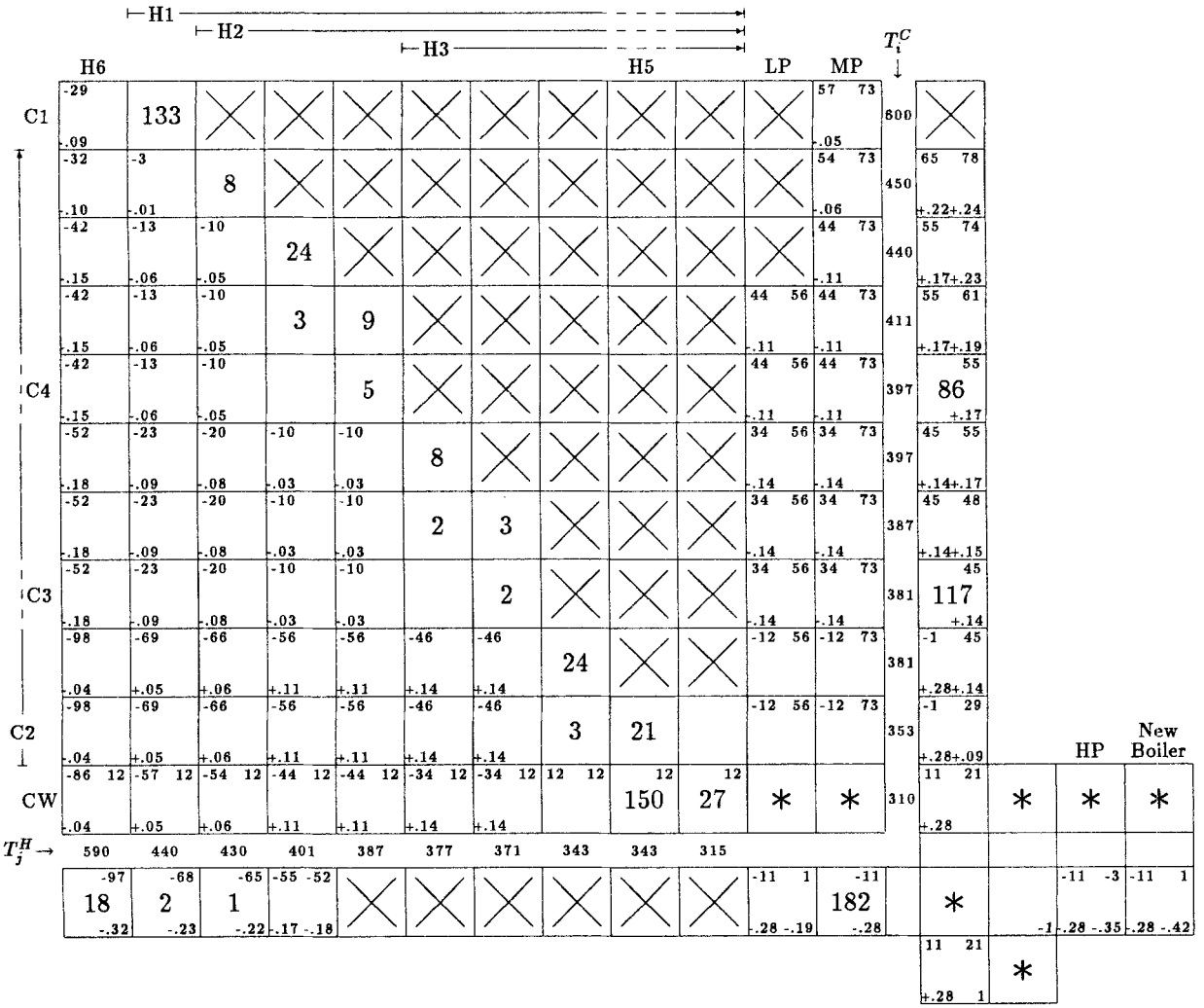

Figure 7. Example 1 at end of "primal phase."

pump systems. Table 3 shows available utilities and their costs; Table 2, the variable cost components of the capital investment.

Example 1

This example from Papoulias and Grossmann (1983b), called the "ABCDE" process, represents a large synthesis loop. The process stream heating and cooling requirements are shown in Table 4. Assuming a minimum combined approach temperature of 10 K, 15 temperature intervals result, where each of the five latent heat loads is given its own interval. To reduce the size of the corresponding array, the intervals above 590 K (for C1) and below 325 K (for H1, . . . , H4) are omitted, since these duties must be met by utilities in any case.

Capital cost contributions are included according to Table 2. Heat exchanger costs are included only for the cooling utility matches and heat engine input cells, to account just for the *difference* in exchanger requirements due to the engine flows. Heat engine inputs below 400 K are disallowed here since the simple turbine cost in Table 2 will not apply at low pressures, and applicable costs make these inputs uneconomical. Work coefficients and cell entries c'_{ij} are computed from Eq. 5 assuming $\eta_s = 0.80$ and $\eta_{ph} = 0.97$. The superheat trajectory is based on initial boiler conditions of 811 K and 200 bar, with $\hat{T}$ values obtained from Figures 3 and 4. Efficiency penalties for moisture have been ignored.

Figure 6 displays the starting array after initial allocation. Note the entry of 0 for W_{out} to "complete" the sum for the Q_i^C column and to satisfy the initial heat balance for the engine system. The two right-most columns are included to consider engine inputs from the available HP steam and a postulated new boiler, respectively. Cost coefficients are based on the initial estimate of $w = -c_{out}^W + c^{Util,J_0} = 341$ \$/kW.

Figure 7 shows the array obtained at the end of the "primal phase." A value of -26.4 MW is obtained for the quantity S, and a single pass of the "dual phase" adjusts to $w = 328$ \$/kW, completing the solution. The flow reversal test is satisfied.

Figure 8 displays the solution array with the optimal heat flows. Steam is obtained from the MP steam utility and generated locally in matches with H6 and H1. Letdown turbines are indicated, exhausting all heat into the process. MP steam is available at a price advantage over LP, HP, and new boiler steam, as evidenced by the cost penalties in their corresponding cells. Simplified economic evaluation based on the costs in Tables 2 and 3 shows a utilities cost savings of \$6 × 10^6/yr for an annualized capital cost increase of \$2 × 10^6/yr.

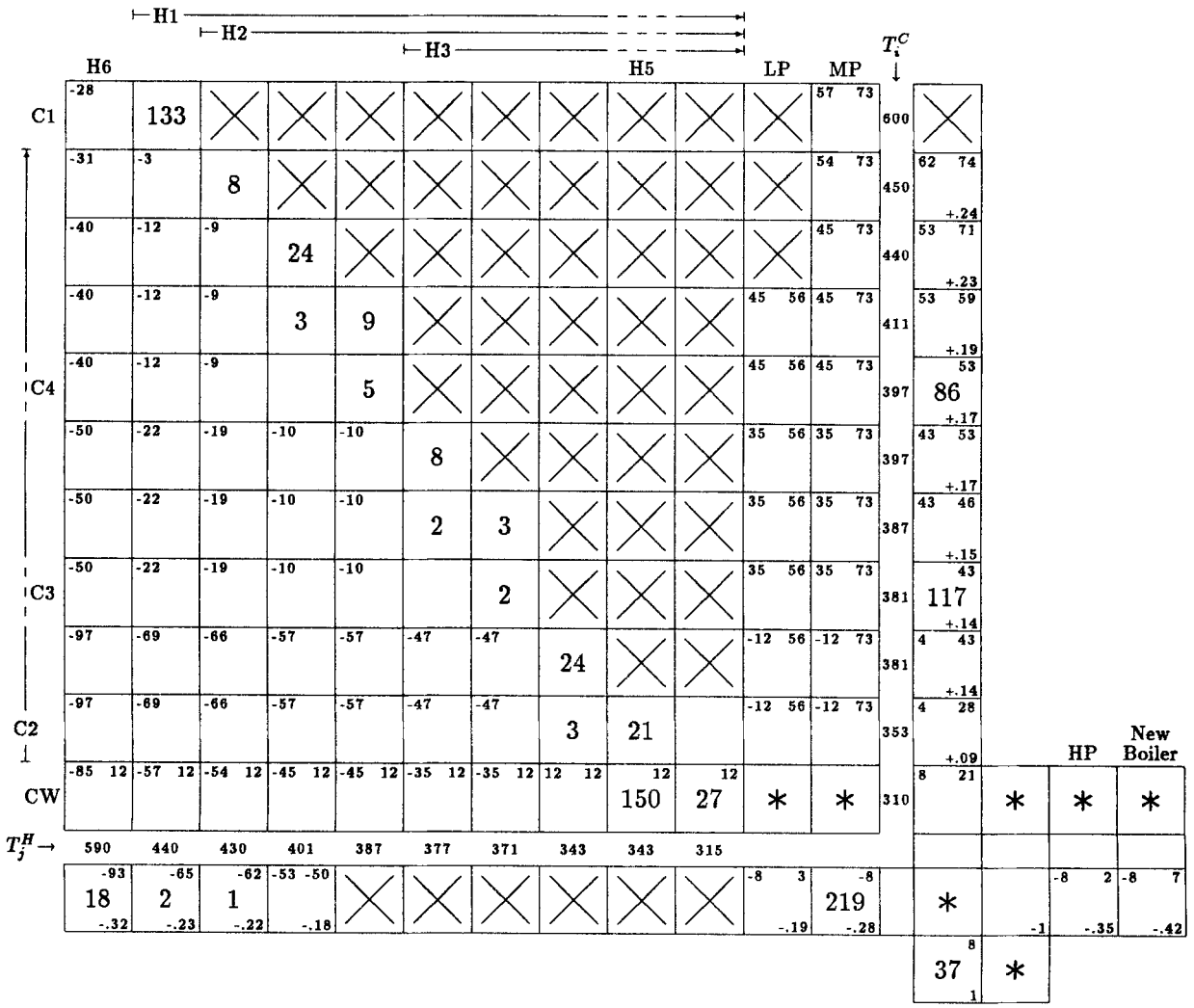

Figure 8. Example 1 array at solution.

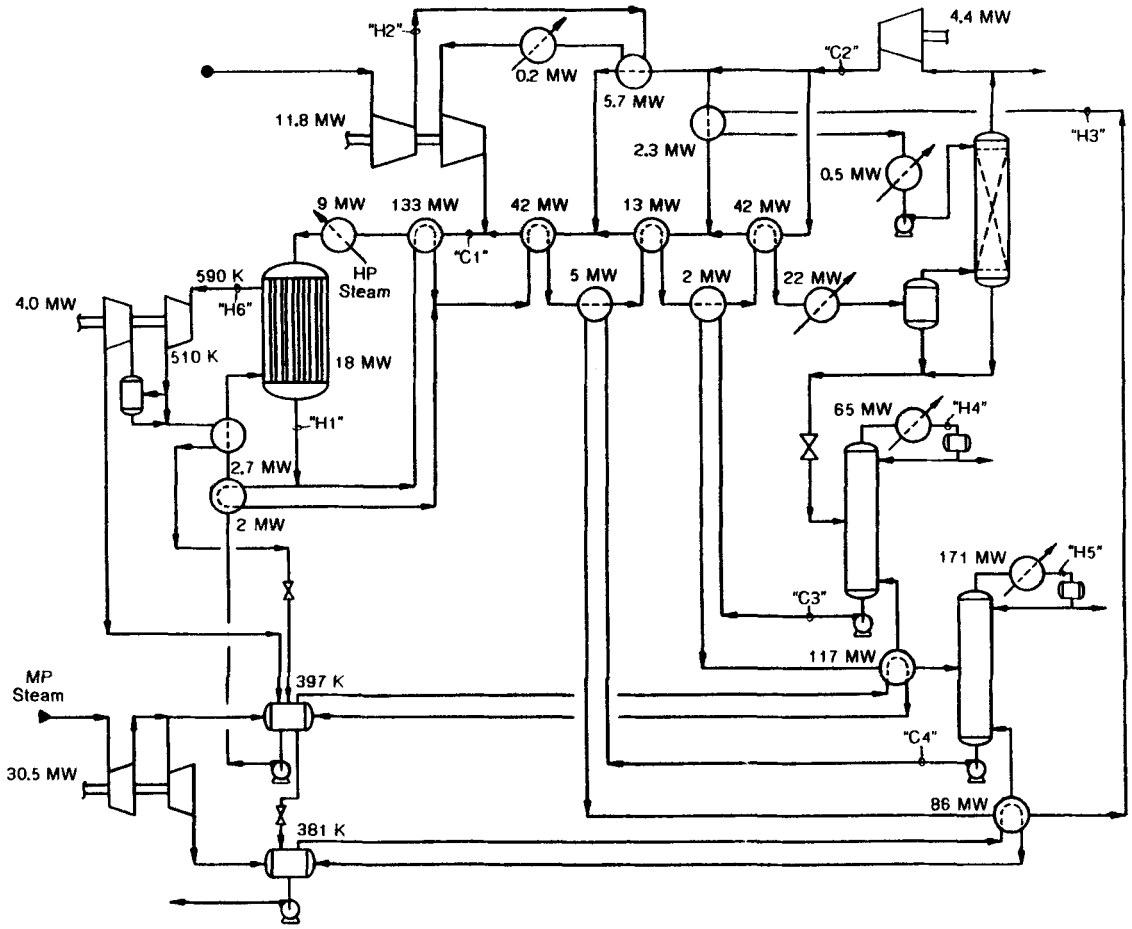

Figure 9. Example 1 solution flowsheet.

Figure 9 presents a flowsheet structure implementing the indicated heat flow scheme. Several aspects of the solution array are of note. No cost will be incurred to shift 21 MW from the H5-C2 match to a H1-C2 match, and this was done, giving a more sensible matching scheme from an operating standpoint, with fewer exchangers. The 1 MW engine input at 430 K was forgone, since the \$9,000 annual penalty indicated in the array to eliminate this match would be more than countered by additional fixed charge components for the match. The 5 MW and 2 MW H1-reboiler matches would cost \$57/kW and \$47/kW annually to eliminate, and should probably be retained if they are acceptable operationally. Not shown in Figure 8, but easily added, would be the cost coefficients for potential organic Rankine cycles operating from inputs below 400 K.

Example 2

This example, based on the ethylene-propylene distillation sequence presented by Colmenares and Seider (1987), illustrates integration with refrigeration/heat pump systems.

Table 5 lists the required process heating and cooling loads. Capital costs are assigned to the heat pump cells according to Table 2, with a cost for additional heat exchange assigned to the heat pump-cooling water match. Work coefficients and c'_{ij} were computed from Eq. 9 with $m = 1.44$ based on $\eta_I = 0.80$, $\eta_R = 0.85$, and $\rho = 1.111$. A combined approach $\Delta T_{\min}$ of 4 K is employed, with $T_0 = 310$ K for the cooling water.

Figure 10 shows the initial allocation. In this problem, it is necessary to use the heat pump cells from the beginning to achieve feasibility. Note the entry of 1,224 to establish the initial overall heat balance on the heat pump system. Cost coefficients were computed from an initial estimate of $w = c_{in}^{W} + c^{\text{Util./o}} = \$461/\text{kW}$.

Figure 11 shows the array obtained after completing the Primal and Dual Phases but prior to the flow reversal check. At this point the flow reversal check detects that the array as shown implies a net flow "backwards" through the heat pump between 321 K and 310 K. Violation of this heat pump "pinch" is corrected by partitioning the heat pump system above and below these temperatures into two systems as shown in Figure 12. This array shows the solution after completing the "dual phase," where the separate multipliers $w_1 = \$461/\text{kW}$ and $w_2 = \$471/$

Table 5. Heating and Cooling Requirements for Example 2

Stream	Initial Temp. K	Final Temp. K	Duty kW
H1	262	262	401
H2	244	244	823
H3	325	325	4,285
C1	341	341	871
C2	270	270	759
C3	336	336	4,230

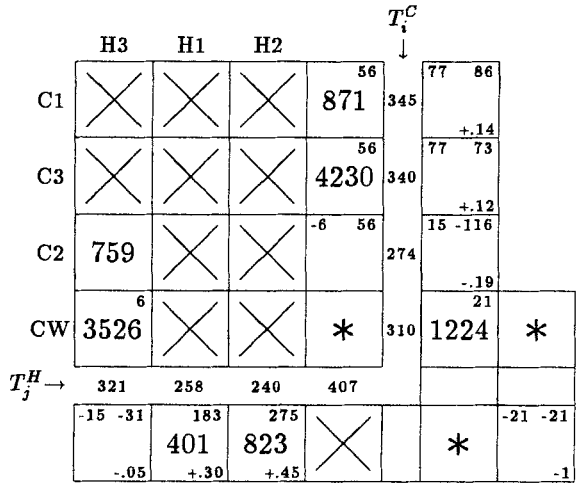

Figure 11. Example 2 at end of "dual phase."

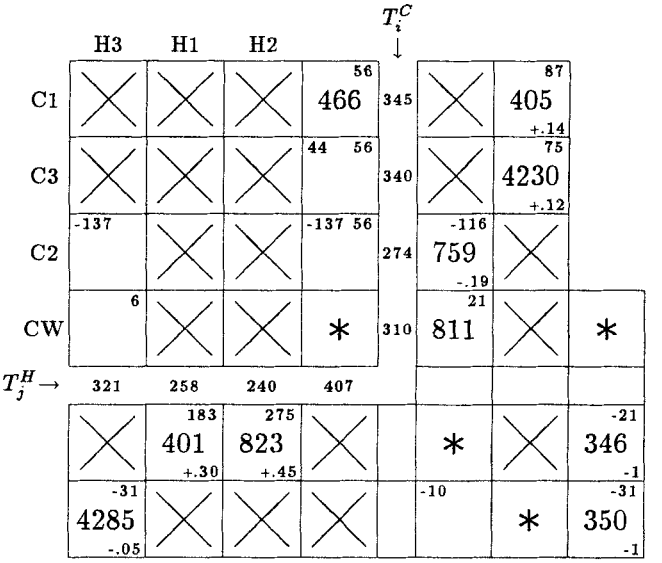

Figure 12. Example 2 solution array with partitioned heat pumps.

kW result for the two systems. Since the linking cell is inactive, two separate heat pump systems are indicated with no cascading of heat between them.

Figure 13 shows preliminary designs for the two heat pump systems, with propylene chosen as refrigerant for the lower temperature cycles and butane used for the higher temperature system. The heat input and rejection flows at different temperature levels are easily accommodated within the compound cycle structure. In the solution array, the entries $p = (\xi - c) = -\$10/\text{kW}$ for the cascading cell suggest that the savings in exchanger cost will not be enough to justify pumping heat up past the cooling water temperature level. The cost to shift loads out of the superambient heat pump begins at \$6/kW, indicating that this aspect of the design is advantageous, although a more rigorous economic evaluation may be in order.

Conclusions

The transportation array formulation offers a suitable and convenient framework for the integral design of heat engines, refrigeration systems, and heat pumps with process heat recovery and utility utilization schemes. The procedure determines the optimal underlying heat flow pattern from basic economic criteria. The results provide a definitive guide in selecting the final system design scheme and implementation. Relevant options requiring detailed examination are indicated, allowing final decisions on specific equipment topology to be made in consideration of additional factors such as operability, maintainability, safety, and physical layout.

The approach is intended to serve as a guide in the preliminary stages of design. Later, more detailed design optimization procedures could be brought to bear on, for instance, the heat

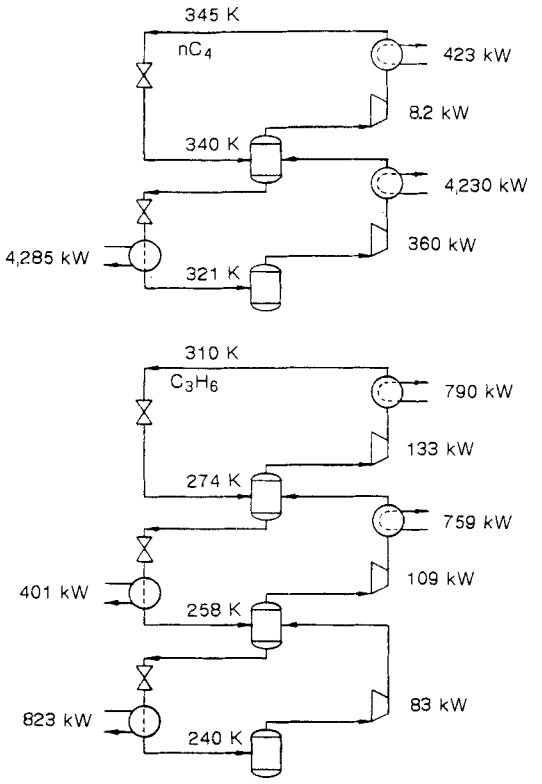

Figure 13. Example 2 solution heat pump systems.

exchanger configuration or the refrigeration system design, if indeed sufficiently accurate cost estimation procedures are available. The procedure presented here has the advantage of comparative simplicity. An interactive computer implementation will provide very convenient application, and it may even be executed by hand (as was done for the examples shown here). It also has the important advantage of retaining designer involvement in the decision process, assuring that the bases for design decisions are understood and validated.

The framework is fairly flexible, and extensions to the basic applications demonstrated here are possible. For instance, situations with an internal power demand that must be supplied in the presence of external power purchase and sale options are easily handled by the inclusion of an additional row with one cell for power production and another for power purchase. The basic representation for heat engine/pump integration presented could also be utilized with a MILP formulation, allowing fixed charge cost components to be treated explicitly.

Acknowledgment

The author would like to thank T. R. Colmenares and W. D. Seider for their helpful comments on this manuscript.

Notation

a = cold stream composite interval heat duty
b = thermodynamic availability function; hot stream composite interval heat duty
c = cell cost coefficient
f = adjustment factor
F = flowrate of working fluid
h = enthalpy per unit mass
ΔH = stream interval heat duty
k = capital cost coefficient
p = cell penalty cost
P = pressure
q = cell heat flow; vapor fraction
Q = heat flow in/out of heat engine/pump system
s = entropy per unit mass
S = slack quantity
t = tie variable between engine/pump input and output balances
T = temperature
$\hat{T}$ = Carnot equivalent temperature
U = limit on work import or export
w = work cost multiplier
W = work input or output

Greek letters

ξ = cell multiplier sum
γ = column multiplier
η = efficiency
ρ = temperature level ratio; row multiplier
ζ = work coefficient

Subscripts

c = cycle efficiency relative to reversible
H = for differential expansion
I = compressor isentropic efficiency
ph = accounting for real preheat system
R = for Rankine cycle topology
s = accounting for turbine and pump efficiencies
sat = point where steam trajectory reaches saturation
0 = process rejection sink

Superscripts

C = rejection from heat engine/pump to cold stream
H = input to heat engine/pump from hot stream
L = condensate conditions at P
Util = utility unit cost
V = steam conditions at P

Literature Cited

Cerda, J., A. W. Westerberg, D. Mason, and B. Linnhoff, "Minimum Utility Usage in Heat Exchanger Network Synthesis. A Transportation Problem," *Chem. Eng. Sci.*, **38**(3), 373 (1983).

Cerda, J., and A. W. Westerberg, "Synthesizing Heat Exchanger Networks Having Restricted Stream/Stream Matches Using Transportation Problem Formulations," *Chem. Eng. Sci.*, **38**(10), 1723 (1983).

Colmenares, T. R., and W. D. Seider, "Heat and Power Integration of Chemical Processes," *AIChE J.*, **33**(6), 898 (1987).

Colmenares, T. R., and W. D. Seider, "Synthesis of Utility Systems Integrated With Chemical Processes," *Ind. Eng. Chem. Res.*, **28**, 84 (1989).

Gundersen, T., and L. Naess, "The Synthesis of Cost Optimal Heat Exchanger Networks," *Comp. & Chem. Eng.*, **12**(6), 503 (1988).

Murty, K. G., *Linear Programming*, Wiley (1983).

Papoulias, S. A., and I. E. Grossmann, "A Structural Optimization Approach in Process Synthesis: II. Heat Recovery Networks," *Comp. & Chem. Eng.*, **7**(6), 707 (1983).

Papoulias, S. A., and I. E. Grossmann, "A Structural Optimization Approach in Process Synthesis: III. Total Processing Systems," *Comp. & Chem. Eng.*, **7**(6), 723 (1983).

Townsend, D. W., and B. Linnhoff, "Heat and Power Networks in Process Design," *AIChE J.*, **29**(5), 742 (1983).

Appendix A

1. In Eq. 3, the turbine efficiency η_{turbine} assumed to be constant is the overall isentropic efficiency, whereas Figure 3 assumes a constant differential expansion efficiency η_H. Strictly, these assumptions are not equivalent, and if one efficiency is constant over the trajectory, the other must vary in a predetermined manner. The approximation involved is acceptable for the purpose intended here, remembering that the two efficiencies will differ numerically. The relationship between the two efficiencies may be approximated with

$$\eta_{\text{turbine}} = \frac{1 - \dfrac{T_0}{T}}{1 - \left(\dfrac{T_0}{T}\right)^{1/\eta_H}} \tag{36}$$

Although simply using a mean value for η_{turbine} will usually be adequate, Eq. 5 may be used with a schedule of efficiencies varying with temperature level if desired.

2. Moisture content will reduce the efficiencies of the wet turbine stages somewhat. One rule-of-thumb estimate for this effect is $\eta_{\text{wet}} = q \cdot \eta$ where q = vapor fraction; the trajectories in Figure 3 employ this estimate. This adjustment may be applied, if desired, to Eq. 5, yielding $\zeta_{\text{adjusted}} = \bar{q}\zeta$ for wet conditions and $\zeta_{\text{adjusted}} = \zeta - (1 - \bar{q}_{\text{sat}})\,[(1 - \zeta)/(1 - \zeta_{\text{sat}})]$ for superheated conditions. ζ_{sat} is evaluated at T_{sat}, and estimates $\bar{q} = \frac{1}{2}(q + q_0)$ and $\bar{q}_{\text{sat}} = \frac{1}{2}(1 + q_0)$, with q_0 evaluated at T_0.

Appendix B

The following approximate expressions are convenient for estimating $\hat{T}$ for steam systems given the heat input or rejection temperature. The location of the steam expansion trajectory is established by the value of T_{sat}, the temperature at which the trajectory reaches saturation and moisture begins. The value of

T_{sat} that will result in a specified vapor fraction q at temperature T may be obtained from

$$T_{sat} \doteq T + \frac{T_b}{2\phi} \ln\left[\left(\frac{\phi - 1}{\phi + 1}\right)\frac{\phi q + 1}{\phi q - 1}\right] \tag{37}$$

where

$$\phi = \left(\frac{\eta_H T_b}{T_a}\right)^{1/2}, \; T_a = 380 \text{ K}, \; T_b = 1{,}300 \text{ K}$$

For heat input at $T^H = T$, the corresponding condensation temperature T^L is first estimated from

$$\frac{1}{T^L} \doteq \frac{1}{T_{sat}} - \frac{1}{\eta_H T_{\lambda_1}} \ln \frac{T}{T_{sat}}$$

$$T_{\lambda_1} = 1{,}170 \text{ K} \tag{38}$$

Then $\hat{T}$ is obtained from

$$\hat{T} \doteq T^L \left[\frac{T - T^L + T_\lambda}{T^L \ln \dfrac{T}{T^L} + T_\lambda}\right] \tag{39}$$

where

$$T_\lambda = T_{\lambda_0}(1 - T^L/T_{crit})^{3/4}, \; T_{\lambda_0} = 2{,}250 \text{ K}, \; T_{crit} = 647.13 \text{ K}$$

For heat rejection at $T^C = T^L$, Eq. 38 is used instead to estimate the corresponding steam temperature T. Then $\hat{T}$ is obtained from Eq. 39.

The above relations cannot not be relied upon for high accuracy, but they can be useful for preliminary design purposes.

Manuscript received Aug. 15, 1988, and revision received Feb. 27, 1989.